Available online at www.sciencedirect.com
SCIENCE DIRECT®
Journal of Solid State Chemistry 179 (2006) 1022–1028
JOURNAL OF SOLID STATE CHEMISTRY
www.elsevier.com/locate/jssc

New insight into the symmetry and the structure of the double perovskites Ba_2LnNbO_6 (Ln = lanthanides and Y)

W.T. Fu*, D.J.W. IJdo

Gorlaeus Laboratories, Leiden Institute of Chemistry, Leiden University, P.O. Box 9502, 2300 RA Leiden, The Netherlands

Received 28 October 2005; received in revised form 12 December 2005; accepted 17 December 2005
Available online 25 January 2006

Abstract

Structures of the double perovskites Ba_2LnNbO_6 (Ln = La, Pr, Nd, Sm, Eu, Tb, Dy, Ho, and Y) at room temperature have been re-examined by Rietveld profile analysis of X-ray diffraction data. It was shown that the correct phase sequence across the lanthanides is $I2/m$ (Ln = La, Pr, Nd, and Sm), $I4/m$ (Ln = Eu, Gd, Tb, and Dy), and $Fm\bar{3}m$ (Ln = Ho and Y), respectively. All phases can be derived from the ideal cubic perovskite by ordering the Ln(III) and Nb(V) ions and by out-of-phase tilting the LnO_6/NbO_6 octahedra around either the primitive two-fold $[110]_p$-axis ($I2/m$) or the four-fold $[001]_p$-axis ($I4/m$). The monoclinic $P2_1/n$ structure that contains both out-of-phase and in-phase tilt around the primitive $[110]_p$- and $[001]_p$-axis, respectively, has not been observed for this series of compounds.

Keywords: Perovskites; X-ray powder diffraction; Crystal structures

1. Introduction

In recent years, the structural and physical properties of the double perovskites Ba_2LnMO_6, Ln = lanthanide and Y, M = Nb, Ta, and Sb, have been investigated as the new substrate materials of high-T_c superconductors [1] and for the possible use as high-temperature protonic conductors [2]. The series of the compounds Ba_2LnNbO_6 was first reported by Brixner [3] to have a simple cubic perovskite structure with the exception of Ba_2LaNbO_6, which he described as a tetragonally distorted perovskite. A rhombohedral distortion of this compound was also reported [4]. Von Wittmann et al. [5] referred the unit cell of Ba_2LaNbO_6 as monoclinic and that of Ba_2GdNbO_6 as tetragonal, respectively. Evdokimov and Men'shenina [6] determined the monoclinic unit cells for Ln = La–Sm, the tetragonal unit cells for Ln = Eu–Tb, and double cubic unit cells for Ln = Dy–Lu and Y. In all above-mentioned works, no structural details were given. More recently, Hemni et al. [7] carried out the Rietveld analyses of the X-ray diffraction data and described the structure of Ba_2LnNbO_6 (Ln = La–Lu), all in the space group $P2_1/n$ (tilt system ($a^-a^-c^+$)) with the unit cell of $a \approx b \approx \sqrt{2}a_p$, $c \approx 2a_p$, and $\beta \approx 90^\circ$, where a_p denotes the lattice constant of the primitive cubic perovskite. In their published work, only the refined atomic positions of Ba_2PrNbO_6 were listed, and those of the other compounds were mentioned to be comparable. However, considering the systematic change of the ionic radius of lanthanides [8], such a description seems to be questionable. For example, the tolerance factor of Ba_2LnNbO_6, defined as $t = (r_{Ba} + r_O)/\sqrt{2}(\bar{r}_{(Ln,Nb)} + r_O)$ with $\bar{r}_{(Ln,Nb)}$ being the averaged ionic radius of the Ln and Nb cations, varies from 0.952 (Ln = La) to 0.99 (Ln = Lu). It is rather unexpected that the whole series adopts the same space group. In particular, the compounds with the heavier lanthanides are expected to have higher symmetry in view of their tolerance factors being closer to unity. In fact, the X-ray diffraction pattern of Ba_2TmNbO_6, the only one shown in Ref. [7], showed no superlattice reflection associated with the in-phase tilting of octahedra. In addition, no peak splitting, except the apparent $K\alpha_1$ and $K\alpha_2$ splitting, that might suggest the symmetry being lower than cubic can be seen. Further, the refined oxygen positions of Ba_2PrNbO_6 all showed quite larger standard deviations, indicating that the space group $P2_1/n$ could possibly be inappropriate.

*Corresponding author. Fax: +31 71 5274537.
E-mail address: w.fu@chem.leidenuniv.nl (W.T. Fu).

0022-4596/$ - see front matter © 2005 Elsevier Inc. All rights reserved.
doi:10.1016/j.jssc.2005.12.031

In the recent investigations on the structures of the double perovskite families with the formula Ba_2LnMO_6, Ln = lanthanide and Y, M = Ir, Ru, and Sb, we showed that the monoclinic symmetry ($P2_1/n$) once reported for these compounds is actually incorrect: Ba_2LaIrO_6 [9], Ba_2LaRuO_6 [10], and Ba_2LnSbO_6 (Ln = La, Pr, and Nd) [11] all have rhombohedral symmetry with the space group $R\bar{3}$. Further, all three series showed the symmetry change from rhombohedral ($R\bar{3}$) to cubic ($Fm\bar{3}m$) when the ionic radius of Ln ions is decreased. Clearly, the space group $R\bar{3}$ falls into the Glazer's classification of the tilt systems [12] for ordered double perovskites (tilt system ($a^-a^-a^-$)) [13], and the phase sequence, $R\bar{3} \rightarrow Fm\bar{3}m$, is a logical one as was expected from the recent group-theoretical analysis [14]. Given that the ionic radius of Nb(V) (0.64 Å) is somewhat larger than, but comparable to, those of Sb(V) (0.60 Å), Ir(V) (0.57 Å), and Ru(V) (0.565 Å), it is interesting to confirm whether the monoclinic symmetry indeed occurs in the series of Ba_2LnNbO_6 (Ln = lanthanides and Y), and, if it does, whether the correct space group should be $I2/m$ [14] rather than $P2_1/n$ [7]. In addition, the reported tetragonal phase [5,6] might have the space group $I4/m$ [13,14], corresponding to a tilting of the octahedra around the primitive four-fold axis (tilt system ($a^0a^0c^-$)). The phase sequence in Ba_2LnNbO_6 is then different from those in Ba_2LnMO_6 (M = Ir, Ru, and Sb). Therefore, we carried out a systematic X-ray powder diffraction study on the crystal structure of Ba_2LnNbO_6, and report the new results in this paper.

2. Experimental

Samples of Ba_2LnNbO_6 (Ln = La, Pr, Nd, Sm, Gd, Tb, Dy, and Y) were prepared from $BaCO_3$, La_2O_3 Pr_6O_{11}, Nd_2O_3, Sm_2O_3, Eu_2O_3, Gd_2O_3, Tb_4O_7, Dy_2O_3, Y_2O_3, and Nb_2O_5 in alumina crucibles using the standard solid-state reaction in air. The hygroscopic La_2O_3 and Nd_2O_3 were preheated at 1000 °C for several hours before use. The mixtures were first heated at 1100 °C overnight. The resultant powders were then reground and sintered with a temperature step of 100 °C and 20 h in each step. The final reaction temperature was 1350 °C. The samples were furnace cooled to room temperature.

X-ray diffraction patterns were collected with a Philips PW1050 diffractometer using Cu$K\alpha$ radiation in steps of 0.02° (2θ) and 12 s counting time in the 2θ range between 10° and 117°.

Model refinements were performed by the Rietveld method [15] using the Rietica computer program [16]. A polynomial function with six parameters was used to fit the background. The profiles have been fitted using a pseudo-Voigt function with peak asymmetric correction.

3. Results

X-ray powder diffraction patterns of some selected Ba_2LnNbO_6 compounds at room temperature are shown in Fig. 1. All are dominated by the lines strongly resembling the primitive cubic perovskite. For compounds with light lanthanides, many of the main diffraction lines are, however, clearly split, indicating that their symmetries are lower than cubic. Since the scattering powers to X-ray of Ln and Nb atoms are quite close, the superlattice diffraction lines arising from their ordering are of low intensity. But a few of the weak additional lines (indicated by asterisks in Fig. 1) are visible, signifying the presence of a supercell in these compounds.

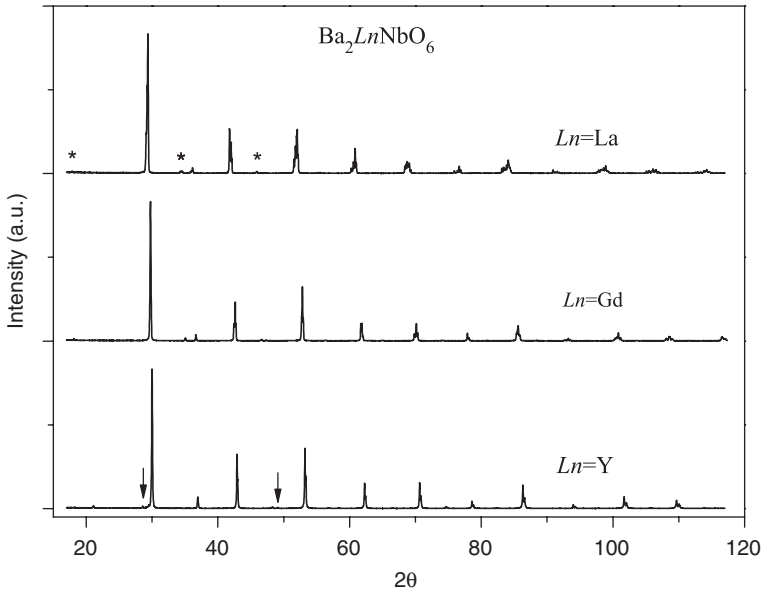

Fig. 1. X-ray powder diffraction patterns of Ba_2LnNbO_6 (Ln = La, Gd, and Y). Some visible superlattice reflections are marked by asterisks. For Ln = Y, a few very weak peaks due to trace of the $Y_3NbO_7/YNbO_4$ contaminations can be seen as indicated by the arrows.

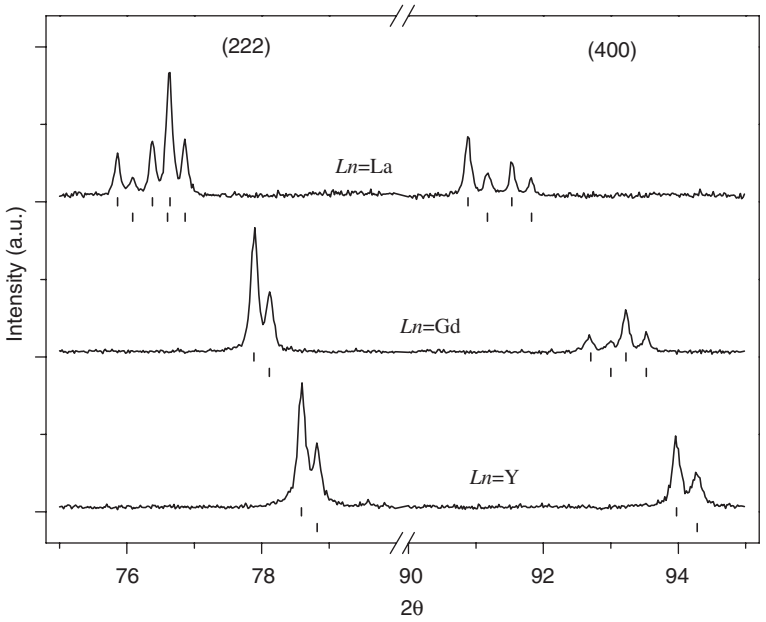

Fig. 2. An enlarged section of the diffraction patterns of Ba_2LnNbO_6 with Ln = La, Gd, and Y showing the basic (222) and (400) reflections. The tick marks below are the calculated positions of the Bragg's reflections using the refined lattice parameters in the space groups $I2/m$ (Ln = La), $I4/m$ (Ln = Gd), and $Fm\bar{3}m$ (Ln = Y), respectively. The significance of the peak splitting due to the octahedral tilt around the principle axes of the primitive cell is discussed in the text.

To identify the exact symmetries and the associated space groups, we examined both the occurrence of superlattice diffraction lines and the splitting of the main diffraction peaks that correspond to the basic cubic perovskite cell. In all Ba_2LnNbO_6, the observed superlattice diffraction lines are indexed in terms of a double-edge unit cell with the odd–odd–odd indices. Such indexing suggests the only possibility of the out-of-phase tilting of the octahedra, if it exists at all. The reported space group $P2_1/n$ [7] that allows the in-phase octahedral tilt about the four-fold axis of the primitive cubic cell is thus unlikely to occur. Considering the specified symmetries in the literatures [4–6], i.e. monoclinic, rhombohedral, tetragonal, and cubic, it leads to the following possible space groups [13,14]: $I2/m$ ($a^-a^-c^0$), $R\bar{3}$ ($a^-a^-a^-$), $I4/m$ ($a^0a^0c^-$), and $Fm\bar{3}m$ ($a^0a^0a^0$), for which the last one contains no octahedral tilting. Inspecting the splitting of main diffraction peaks has shown that the samples of Ba_2LnNbO_6 with Ln = La, Pr, Nd, and Sm adopt the monoclinic symmetry (Fig. 2). This can readily be seen from the basic (222) and (400) reflections that split into a triplet and a doublet, respectively, as were expected in the space group $I2/m$. For phases with Ln = Eu, Gd, Tb, and Dy, the basic (222) reflection does not split, but the splitting of the basic (400) reflection remains. The symmetry is, therefore, tetragonal with the likely space group $I4/m$. With further decreasing the ionic radii of Ln, i.e. Ln = Y and Ho, no splitting of the main diffraction lines could be resolved anymore, except that being due to the $K\alpha_1$ and $K\alpha_2$ radiations. Consequently, the space group is cubic $Fm\bar{3}m$. Clearly, the rhombohedral symmetry ($R\bar{3}$) that has been observed in a number of Ba_2Ln(III)M(V)O_6-type perovskites does not occur in present series of compounds. Further, we did not find any evidence that might suggest a triclinic symmetry, e.g. the space groups $P\bar{1}/I\bar{1}$, once reported for Ba_2LaRuO_6 [17].

The structures of Ba_2LnNbO_6 were modelled, using the Rietveld method [15], in the space groups $I2/m$, $I4/m$, and $Fm\bar{3}m$, respectively, with the initial atomic positions taken from those of Ba_2NdBiO_6 ($I2/m$) [18] and of Sr_2MgWO_6 ($I4/m$) [19]. These models could explain satisfactorily all essential features of the observed diffraction profiles. Table 1 summarizes the refined atomic positions and thermal parameters of a few representative Ba_2LnNbO_6. Table 2 lists some selected interatomic distances. The plots of the observed and calculated profiles of the selected samples are shown in Fig. 3.

4. Discussion

The structures of the double perovskites Ba_2LnNbO_6 (Ln = La, Pr, Nd, Sm, Eu, Gd, Tb, Dy, Ho, and Y) can all be derived from the primitive cubic aristotype by ordering the LnO_6 and NbO_6 octahedra, and by tilting the octahedra around one of the principal axis of the cubic cell. In Ba_2LnNbO_6 with Ln = La, Pr, Nd, and Sm, the octahedra are tilted around the two-fold $[110]_p$-axis, resulting in the monoclinic symmetry with the space group $I2/m$. The tilting of the octahedra reduces the c-axis with the reduced cell axes ratio, defined as $a_p(b_p) = a(b)/\sqrt{2}$ and $c_p = c/2$, being $c_p/a_p(b_p) < 1$. The magnitude of the averaged tilt angles, calculated from the refined oxygen coordinates

Table 1
Refined lattice parameters and atomic positions of some selected Ba_2LnRuO_6 in the space groups $I2/m$, $I4/m$, and $Fm\bar{3}m$, respectively

$I2/m$				$I4/m$				$Fm\bar{3}m$	
Ba_2LaNbO_6		Ba_2NdNbO_6		Ba_2GdNbO_6		Ba_2TbNbO_6		Ba_2YNbO_6	
a (Å)	6.14448(8)	a (Å)	6.07918(9)	a (Å)	5.99856(5)	a (Å)	5.98428(5)	a (Å)	8.43159(8)
b (Å)	6.09131(9)	b (Å)	6.04547(9)	c (Å)	8.52004(9)	c (Å)	8.48173(10)		
c (Å)	8.60400(11)	c (Å)	8.53909(13)						
β (°)	90.348(1)	β (°)	90.134(1)						
Ba	4*i* (*x*,0.5,*z*)	Ba	4*i* (*x*,0.5,*z*)	Ba	4*d* (0,0.5,0.25)	Ba	4*d* (0,0.5,0.25)	Ba	8*c* (0.25,0.25,0.25)
x	0.4953(4)	x	0.4981(6)	Gd	2*a* (0,0,0)	Gd	2*a* (0,0,0)	Y	4*a* (0,0,0)
z	0.2516(3)	z	0.2509(4)	Nb	2*b* (0,0,0.5)	Nb	2*b* (0,0,0.5)	Nb	4*b* (0.5,0.5,0.5)
La	2*c* (0.5,0,0)	Nd	2*c* (0.5,0,0)	O(1)	4*e* (0,0,*z*)	O(1)	4*e* (0,0,*z*)	O	24*e* (*x*,0,0)
Nb	2*b* (0,0.5,0)	Nb	2*b* (0,0.5,0)	z	0.269(2)	z	0.271(2)	x	0.2665(7)
O(1)	4*i* (*x*,0,*z*)	O(1)	4*i* (*x*,0,*z*)	O(2)	8*h* (*x*,*y*,0)	O(2)	8*h* (*x*,*y*,0)	B (Å)^2 [a]	0.22(2)
x	0.582(2)	x	0.547(3)	x	0.242(2)	x	0.242(2)		
z	0.280(2)	z	0.276(2)	y	0.300(1)	y	0.292(1)		
O(2)	8*j* (*x*,*y*,*z*)	O(2)	8*j* (*x*,*y*,*z*)	B (Å)^2 [a]	0.56(2)	B (Å)^2 [a]	0.14(2)		
x	0.213(2)	x	0.219(2)						
y	0.250(2)	y	0.266(2)						
z	0.021(1)	z	0.026(1)						
B (Å)^2 [a]	0.52(2)	B (Å)^2 [a]	0.43(2)						
$R_{wp} = 15.22\%$, $R_p = 11.54\%$, $R_B = 5.86\%$, $\chi^2 = 2.28$		$R_{wp} = 13.79\%$, $R_p = 9.71\%$, $R_B = 3.72\%$, $\chi^2 = 2.19$		$R_{wp} = 14.85\%$, $R_p = 10.55\%$, $R_B = 3.21\%$, $\chi^2 = 2.68$		$R_{wp} = 14.40\%$, $R_p = 10.44\%$, $R_B = 4.28\%$, $\chi^2 = 2.46$		$R_{wp} = 15.22\%$, $R_p = 11.11\%$, $R_B = 5.49\%$, $\chi^2 = 2.15$	

[a]The overall thermal parameters were used in the refinements.

Table 2
Selected interatomic distances (Å) in Ba_2LnNbO_6 (Ln = La, Gd, and Y)

	Ba_2LaNbO_6		Ba_2GdNbO_6		Ba_2YNbO_6	
Ln–O(1)	2.461(13)	2 ×	2.294(15)	2 ×	2.247(6)	6 ×
Ln–O(2)	2.338(9)	4 ×	2.316(9)	4 ×		
Nb–O(1)	1.960(13)	2 ×	1.966(15)	2 ×	1.969(6)	6 ×
Nb–O(2)	2.015(9)	4 ×	1.955(10)	4 ×		
Ba–O(1)	2.614(13)	1 ×	3.0038(9)	4 ×	2.9842(3)	12 ×
	3.101(2)	2 ×				
	3.556(14)	1 ×				
Ba–O(2)	2.798(9)	2 ×	2.843(6)	4 ×		
	3.041(13)	2 ×	3.189(7)	4 ×		
	3.068(14)	2 ×				
	3.327(9)	2 ×				

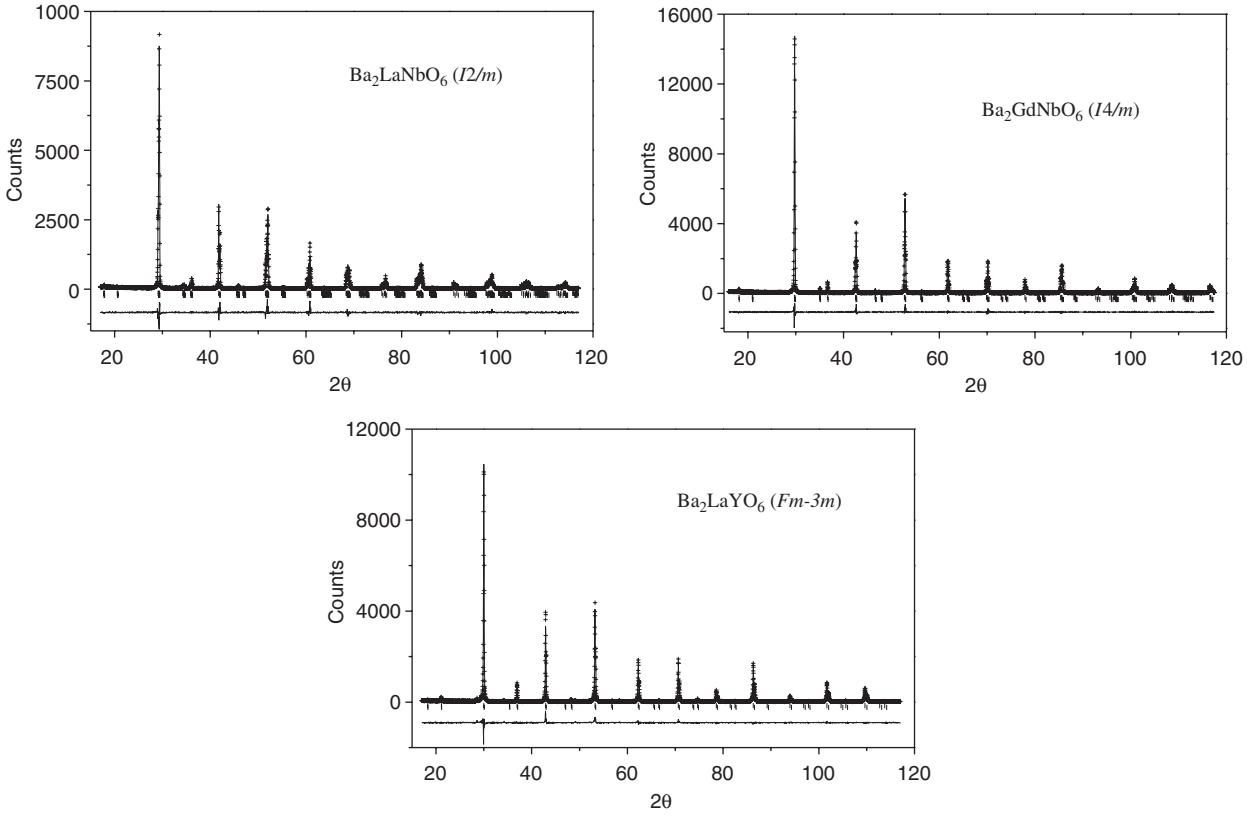

Fig. 3. Observed (crosses) and calculated (full line) profiles of the X-ray powder diffraction for Ba_2LaNbO_6, Ba_2GdNbO_6, and Ba_2YNbO_6. Tick marks below the profiles indicate the positions of the allowed Bragg reflections. A difference curve (observed–calculated) is shown at the bottom of each plot.

using $\varphi_M = 1/3[4(x_{O(1)}-0.5)a/c + 8z_{O(2)}c/a]$ (rad) [20], decreases with decreasing ionic radius of lanthanide (9.0°, 8.2°, 8.0°, and 6.9°, respectively) (Fig. 4), being in agreement with the increase of the tolerance factor (0.952, 0.961, 0.962, and 0.968, respectively). For compounds with Ln = Eu, Gd, Tb, and Dy, the LnO_6/NbO_6 octahedra are tilted around the four-fold $[001]_p$-axis, corresponding to the tetragonal symmetry of the space group $I4/m$. Again, the tilting angle, $\varphi_T = 2[y_{O(2)}-x_{O(2)}]$ (rad) [20], diminishes with increasing the tolerance factor, being 7.0°, 6.6°, 5.7°, and 4.9° for Ln = Eu, Gd, Tb, and Dy, respectively (Fig. 4), and the rotation of octahedra causes the decrease of the a-axis leading to $c_p/a_p > 1$. As the size of Ln further decreases, e.g. Ln = Ho and Y, no octahedral tilting exists any more, and the structure is simple double cubic.

The above-mentioned phase sequence clearly shows the dependence of the crystal structure on the ionic radii, i.e. the tolerance factor. It is that one might expect given the systematic change of the match between the Ba–O and the averaged (Ln,Nb)–O bond lengths. For bigger lanthanides, the undersized Ba cation is too small to fit in the (Ln,Nb)O_3

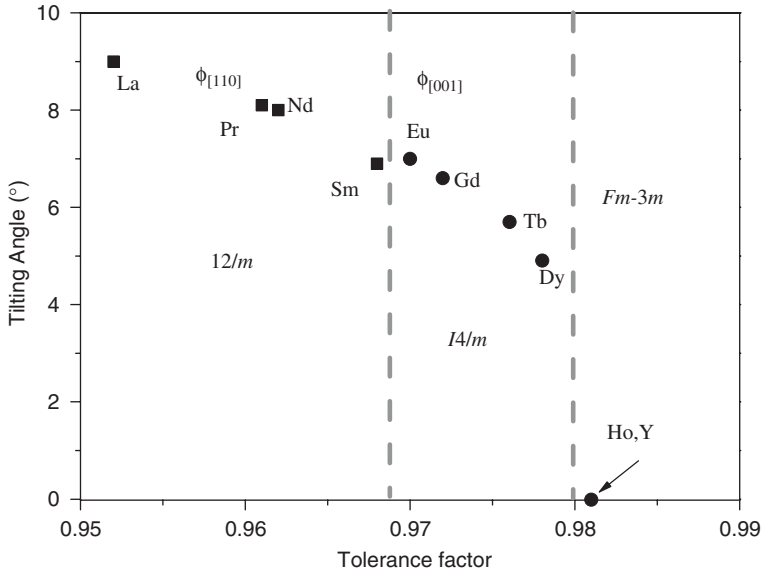

Fig. 4. Calculated tilting angles in Ba_2LnNbO_6 (Ln = La, Pr, Nd, Sm, Eu, Gd, Tb, Dy, Ho, and Y) as the function of the tolerance factor t.

framework. Tilting of the octahedra reduce the size of the cavity by reducing part of the Ba–O distances. In Ba_2LnNbO_6 with $t \leqslant 0.968$, the octahedral tilting around the primitive two-fold $[110]_p$-axis splits the 12 equidistant Ba–O bonds into seven different distances (Table 2): three of them being quite shorter and other three being much longer. The averaged value (3.068 Å for Ln = La) is, however, compatible to that calculated from the sum of Shannon'n ionic radii (3.01 Å) [8]. For compounds with the tolerance factor in the range of $0.968 < t \leqslant 0.978$, the tilting of octahedra about the primitive four-fold $[001]_p$-axis results in three different Ba–O bond lengths. Their differences are relatively small, and the average is, again, in agreement with the sum of ionic radii. On the other hand, the tilting of octahedra does not significantly alter the Nb–O bond distance with the averaged values ranging from 2.02 Å (Ln = La) to 1.97 Å (Ln = Y), respectively (Table 2).

The present investigation confirms the existence of the monoclinic symmetry in Ba_2LnNbO_6, but the space group is found to be $I2/m$ instead of $P2_1/n$ as was previously suggested by Hemni et al. [7]. Since no diffraction lines that associate with the in-phase tilting are present, it does not seem to be logical to adopt the space group $P2_1/n$ for Ba_2LnNbO_6. In fact, the space group $I2/m$ has already been observed in a number of double perovskites: e.g. $Ba_2Bi(III)Bi(V)O_6$ ($t = 0.927$) [21], Ba_2LnBiO_6, Ln = Pr and Nd ($t = 0.936$ and 0.937) [18] and Ba_2SrWO_6 ($t = 0.929$) [22], all having even smaller tolerance factor. It should also be mentioned that the double perovskite Ba_2SrUO_6 does adopt the monoclinic $P2_1/n$ structure as, apparently, a consequence of its too small tolerance factor, $t = 0.904$ [23].

Our results are in agreement with the earlier finding of Evdokimov and Men'shenina [6], who reported the correct lattice parameters and the unit cells for Ba_2LnNbO_6. The only exception is the tetragonal Ba_2DyNbO_6, which they described as double cubic. In their published works, the unit-cell parameters of the related double perovskites Ba_2LnTaO_6 were also given showing the same behavior as the Nb counterpart. Very likely, the phase sequence of Ba_2LnTaO_6 is the same as the title compounds.

The experiments of Meng and Vitar [2] showed that the double perovskites Ba_2LnNbO_6 could be prepared by a conventional calcination process ($T \approx 1250$ °C), as well as by the molten salt method at the temperature range of 300–500 °C, except those of Ln = La and Nd, which could not be prepared by the later method. In addition, powders of Ba_2LaNbO_6 and Ba_2NdNbO_6 formed by high-temperature calcination process were found to readily decompose when introduced in the molten salt bath; the analysis of the X-ray diffraction showed the presence of BaO and $LaNbO_4$, respectively, in the bath residue. The authors concluded, therefore, that these compounds are thermodynamically unstable at the temperature of the salt bath, i.e. 350 °C, and their low thermal stability was attributed to the low value of the tolerance factor. However, such a conclusion does not seem to be correct. As was shown by the present investigation, the decrease of the tolerance factor in Ba_2LnNbO_6 leads to the tilting of the octahedra, which results in the lower symmetry. In fact, annealing the Ba_2LaNbO_6 and Ba_2NdNbO_6 in air at the temperature of about 350 °C, we did not observe any trace of decomposition. Also boiling the Ba_2LaNbO_6 powder in water for 1 week, the same authors found that the perovskite structure remains unaffected [2]. These facts strongly suggest that the double perovskites Ba_2LnNbO_6 with Ln = La and Nd are thermodynamically stable at low temperature; they are unstable only in the molten NaOH–KOH bath.

It is interesting to review the occurrence of the tetragonal $I4/m$ structure (tilt system ($a^0a^0c^-$)) in Ba_2LnNbO_6 with Ln = Eu, Gd, Tb, and Dy ($0.968 < t \leqslant 0.978$). In our recent studies on the structure of the Ba_2Ln(III)M(V)O_6-type double perovskites (M = Ru, Ir, and Sb), we observed the rhombohedral $R\bar{3}$ structure with the comparable values of the tolerance factor: i.e. Ba_2LaIrO_6 ($t = 0.968$) [9], Ba_2LaRuO_6 ($t = 0.967$) [10], and Ba_2LnSbO_6 (Ln = La, Pr, and Nd; $t = 0.96-0.971$) [11]. The same structure was also found in double perovskites with somewhat smaller tolerance factor: e.g. Ba_2BiSbO_6 ($t = 0.961$) [24], Ba_2YbBiO_6 ($t = 0.961$) [18], and Ba_2BiTaO_6 ($t = 0.952$) [25]. Although the space group $I4/m$ has previously been found in some double perovskites containing Sr, e.g. Sr_2MWO_6 M = Mg, Ni, and Sr_2CaWO_6 at higher temperature [19], it has not been, to our knowledge, reported in those containing Ba thus far. In a study of the structure stabilizing force in simple ABO_3-type perovskites [26], Woodward has shown that the rhombohedral ($a^-a^-a^-$) tilt system results, as compared to other tilt systems, in the highest coulomb attraction between ions, but it maximizes, at the same time, the repulsive energy as well. Therefore, when A-cation is highly charged with small to moderate tilting angles, i.e. the relatively small deviation of the tolerance factor from unity, the rhombohedral structure can be stabilized because the attractive term overweighs the repulsive term. This conclusion seems to nicely explain the fact that the rhombohedral structure is often observed in the A(III)B(III)O_6-type perovskites, but rarely occurs in the A(II)B(IV)O_3-type perovskites [26]: the tetragonal structure of the ($a^0a^0c^-$) tilt system appears to be the favorable one, e.g. $BaTbO_3$ ($t = 0.985$) [27]. Interestingly, in the related Ba_2Ln(III)M(V)O_6-type double perovskites, the rhombohedral ($a^-a^-a^-$) tilt system is highly preferred. The tetragonal $I4/m$ structure observed in double perovskites containing Sr might be due to the increased covalent A–O bonding. As was also pointed out by Woodward [26], if the electronegativity of A-cation increases, e.g. from Ba to Sr, the covalent A–O bonding interactions may play a more prominent role. In the ($a^-a^-c^+$) or ($a^0a^0c^-$) tilt system, the first coordination sphere of oxygens is not coplanar that increases the number of A-cation orbitals participating in bonding. This is, however, not the case in either ($a^-a^-a^-$) or ($a^0a^0c^+$) tilt system, in which the oxygens around the A-cation are coplanar. Nevertheless, this argument cannot account for the structural difference between Ba_2LnNbO_6 and Ba_2LnMO_6 (M = Ru, Ir, and Sb), since the A-cations are the same. Obviously, the nature of the M–O bonding plays a role in determining the structure stabilization force. As compared to Nb(V), the electronegativity of Ru(V), Ir(V), and Sb(V) increases making the M–O bonding more covalent. It seems that the increased covalence of the M–O bonding favours the coordination sphere of oxygens around the A-cation that maximizes the coulomb attraction, i.e. the ($a^-a^-a^-$) tilt system. Also in other rhombohedral double perovskites mentioned above, e.g. Ba_2BiSbO_6, Ba_2YbBiO_6, and Ba_2BiTaO_6, the Bi–O bonding is evidently more covalent. However, without the detailed calculations, it is yet unclear whether the nature of the octahedrally coordinated M–O bonding indeed accounts for the structural differences observed in those closely related double perovskites.

In conclusion, we have investigated the crystal structures of the double perovskites Ba_2LnNbO_6 (Ln = lanthanides and Y) using X-ray powder diffraction techniques. They all contain the ordered arrangement of Ln(III)/Nb(V) but with different symmetries. The correct space groups across the lanthanides are found to be $I2/m$, $I4/m$, and $Fm\bar{3}m$, respectively, which is in agreement with the progressive increase of the tolerance factor. This phase sequence is also a logical one expected from the recent group-theoretical analysis [14].

References

[1] J. Kurian, K.V.O. Nair, P.K. Sajith, A.M. John, J. Koshi, Appl. Supercond. 6 (1998) 259.
[2] W. Meng, A.V. Virkar, J. Solid State Chem. 148 (1999) 492.
[3] H. Brixner, J. Inorg. Nucl. Chem. 15 (1960) 352.
[4] V.S. Filip'ev, E.G. Fesenko, Kristallografiya 6 (1961) 770.
[5] U. von Wittmann, G. Rauser, S. Kemmler-Sack, Z. Anorg. Allg. Chem. 482 (1981) 143.
[6] A.A. Evdokimov, N.F. Men'shenina, Russ. J. Inorg. Chem. 27 (1982) 1208.
[7] K. Henmi, Y. Hinatsu, N.M. Masaki, J. Solid State Chem. 148 (1999) 353.
[8] R.D. Shannon, Acta Crystallogr. A 32 (1976) 751.
[9] W.T. Fu, D.J.W. IJdo, J. Alloys Compds. 594 (2005) L5.
[10] W.T. Fu, D.J.W. IJdo, Solid State Commun. 136 (2005) 456.
[11] W.T. Fu, D.J.W. IJdo, J. Solid State Chem. 178 (2005) 2363.
[12] A.M. Gazer, Acta Crystallogr. B 28 (1972) 3384.
[13] P.M. Woodward, Acta Crystallogr. B 53 (1997) 32.
[14] C.J. Howard, B.J. Kennedy, P.M. Woodward, Acta Crystallogr. 59 (2003) 463.
[15] H.M. Rietveld, Acta Crystallogr. 22 (1967) 151.
[16] C.J. Howard, B.A. Hunter, A Computer Program for Rietveld Analysis of X-Ray and Neutron Powder Diffraction Patterns, Lucas Height Research Laboratories, 1998.
[17] P.D. Battle, J.B. Goodenough, R. Price, J. Solid State Chem. 46 (1983) 234.
[18] W.T. Harrison, K.P. Reis, A.J. Jacobson, L.F. Schneemeyer, J.V. Waczak, Chem. Mater. 7 (1995) 2161.
[19] M. Gateshki, J.M. Igartua, J. Phys.: Condens. Matter 16 (2004) 6639.
[20] S. Pei, J.D. Jorgensen, B. Dabrovski, D.G. Hinks, D.R. Richards, A.W. Mitchell, J.M. Newsam, S.K. Sinha, D. Vakmin, A.J. Jacobson, Phys. Rev. B 41 (1990) 4126.
[21] D.E. Cox, A.W. Sleight, Solid State Commun. 19 (1976) 969.
[22] D.E. Cox, J.B. Hastings, W. Thomlinson, Acta Crystallogr. A 40 (1984) C368.
[23] W.A. Groen, D.J.W. IJdo, Acta Crystallogr. C 43 (1987) 1033.
[24] W.T. Fu, Solid State Commun. 116 (2000) 461.
[25] K.S. Wallwork, B.J. Kennedy, Q. Zhou, Y. Lee, T. Voigt, J. Solid State Chem. 178 (2005) 207.
[26] P.M. Woodward, Acta Crystallogr. B 53 (1997) 44.
[27] W.T. Fu, D.J.W. IJdo, J. Solid State Chem. 165 (2002) 393.